NUSANTARA BIOSCIENCE
Vol. 16, No. 1, pp. 1-12
May 2024

ISSN: 2087-3948
E-ISSN: 2087-3956
DOI: 10.13057/nusbiosci/n160101

Geometric morphometric divergence of five populations of *Pampus argenteus* (Euphrasen, 1788) from Malaysian waters

SUZYELAWATI MOHD SHUKRI[1], KHALED BINASHIKHBUBKR[1,2], AHMAD DWI SETYAWAN[3], DARLINA MD NAIM[1,♥]

[1]School of Biological Sciences, Universiti Sains Malaysia. 11800 Pulau Pinang, Malaysia. Tel.+60-46534056, ♥email: darlinamdn@usm.my
[2]Department of Biology, Faculty of Science, Hadhramout University. Mukalla, Yemen
[3]Department of Environmental Science, Faculty of Mathematics and Natural Sciences, Universitas Sebelas Maret. Jl. Ir. Sutami 36A, Surakarta 57126, Central Java, Indonesia

Manuscript received: 13 November 2023. Revision accepted: 11 December 2023.

Abstract. *Shukri SM, Binashikhbubkr K, Setyawan AD, Md Naim D. 2024. Geometric morphometric divergence of five populations of* Pampus argenteus *(Euphrasen, 1788) from Malaysian waters. Nusantara Bioscience 16: 1-12.* Phenotypic variation in fish may indicate different environmental conditions that affect species' growth and maturation rates and result from genetic factors that allow fish to adapt to different environments. Understanding population structure and dynamics is extremely important for establishing sustainable fisheries. Silver pomfret, *Pampus argenteus* (Euphrasen, 1788), is an economically important fish species with extensive geographical distribution from the East China Sea to Southeast Asia, Indian Ocean, Arabian Gulf, and the North Sea. It may represent morphologically distinct populations across their range. The main aim of this study is to use geometric morphometric analysis based on physical characteristics to look into the phenotypic diversity of the species across five different populations in Malaysia. Digital images of 260 mature specimens were captured for further analysis. Principle Component Analysis (PCA) and Multivariate analysis (MANOVA) were used in the intra-population analysis based on the transformed distance. At the same time, the Canonical Variance Analysis (CVA) and the Procrustes ANOVA were utilized to determine the inter-population analysis of *P. argenteus*. The Unweighted Pair Group with Arithmetic Mean (UPGMA) method used to support the analysis has shown that the population is clearly grouped according to homologous body shape. The results show that South, West, and North Coast specimens were grouped while the East Coast and Borneo Island shared in another group. The variations in the body shape of *P. argenteus* occurred in body depth, caudal region, and head orientation. The findings separated the populations into two main groups representing the marine region to which they belong. This present study is the first report on phenotypic variations of *P. argenteus* from Malaysian waters utilizing the geometric morphometric method.

Keywords: Geometric morphometric, *Pampus argenteus*, shape variation, species identification

INTRODUCTION

The preservation of species is imperative to maintain sustainable population levels for each species, thereby securing the persistence of biodiversity for future generations. This becomes especially vital considering the severity of the present circumstances. The preservation of biodiversity resources, particularly commercially valuable fish species that play a crucial role in providing protein for human consumption, necessitates the maintenance of a robust and sustainable ecosystem.

Therefore, to ensure the efficient conservation and management of fisheries resources, it is imperative to possess a comprehensive understanding of the stock structure. This knowledge is crucial as it necessitates the separate management of each stock to maximize the overall yield (Lorenzen et al. 2016). Failure to accurately identify and effectively manage distinct population units results in excessive fishing activities, which can ultimately lead to a significant decline in population numbers (Cooke et al. 2016). To effectively address this and reduce the ongoing decline of fish populations, more sophisticated and effective species identification methodologies have been devised and effectively used to ascertain and differentiate the stock structure of various marine fish species (Chen et al. 2018).

Malaysia has recorded 1,951 species of freshwater and marine fishes belonging to 704 genera and 186 families (Chong et al. 2010). Almost half (48%) are currently threatened to some level, while nearly one-third (27%), mostly from the marine and coral habitats, require urgent scientific studies to evaluate their status (Chong et al. 2010; Binashikhbubkr et al. 2023). The endangerment of fish species in Malaysia, encompassing both freshwater and marine environments, is progressively escalating due to several significant factors. These factors include habitat loss or modification, accounting for 76% of the threat, as well as overfishing and bycatch, contributing to the rest of the issue (Chong et al. 2010).

Silver pomfret, *Pampus argenteus* (Euphrasen, 1788), from family Stromateidae, is Malaysia's economically important fish species. The *P. argenteus* is mostly marine and pelagic and has an extensive geographical distribution from the East China Sea to Southeast Asia, Indian Ocean, Arabian Gulf, and the North Sea (Mohitha 2016). The species is significant in Malaysian fishery sectors and has great value and demand as a protein source. However, Malaysia's *P. argenteus* fishery resource has declined

recently, with the total catch in 2019 being only 839 Metric Tons (MT), compared to 1,041 MT in 2018 (LKIM 2019). Furthermore, the fish caught are generally small, implying that better regular fishing and systematic resource management are required (LKIM 2020).

Environmental or habitat variations affect a species' phenotypic characteristics, including behavior, morphology, and physiology (Idaszkin et al. 2013). Specifically, natural selection and gene mutations affect phenotypic variation in inter and intra-populations, generating new morphotypes to maintain greater adaptation in new environments (Trevisan et al. 2016). As a result, the geographical distribution of a species is clearly represented in the shape variation and phenotypic variance of populations (Franssen et al. 2013). Most previous studies on *P. argenteus* relied on typical and traditional morphometric techniques; for example, Zhang et al. (2017) used sagittal otolith morphology to identify five different *Pampus* species from the Chinese coast; Jawad (2014) conducted successful research on the deformations of *P. argenteus* from the Oman coast of the Arabian Gulf, which is based on the conventional morphology of the fish's caudal fin; Iqbal et al. (2015) investigated the morphometrics of *P. argenteus* in Quetta, Pakistan, and discovered that morphometric features are useful for classifying fish and distinguishing sexual and phenotypic variations among species. In general, Geometric Morphometrics (GM) is the newest method focusing on biological shape analysis, which has changed recently. The creation and adoption of techniques for analyzing the Cartesian coordinates of anatomical landmarks are largely responsible for this shift. GM techniques emphasize keeping geometric information consistent throughout a study and offer effective, statistically potent analyses that easily connect abstract, multivariate findings to the physical structure of the original specimens (MacLeod 2018). GM is a powerful and widely used technique nowadays because the data includes information about spatial relationships and relationships between landmarks and organisms (Trevisan et al. 2012; Idaszkin et al. 2013).

Based on our current understanding, there is a lack of published research examining the morphological distinctions among *P. argenteus* populations in Malaysian waters. Thus, the present study aimed to examine GM's efficacy in distinguishing between five populations of *P. argenteus* found in Malaysian waters by analyzing body size and shape variations.

MATERIAL AND METHODS

Sampling

A total of 260 *P. argenteus* individuals were collected from 13 fish landing sites throughout Malaysia to achieve the optimal sample size (Table 1; Figure 1). All mature *P. argenteus* specimens measuring between 18-28 cm in length were acquired. As shown in Table 1, 11 locations from Peninsular Malaysia representing the East Coast (EC), West Coast (WC), North Coast (NC), and South Coast (SC), and two locations from Sabah and Sarawak representing the Borneo Island (BI) were selected in this study. Sampling activities were carried out between March and December 2019 in several locations identified as follows:1. Batu Maung, Penang, 2. Kuala Muda, Kedah, 3. Kuala Perlis, Perlis, 4. Tok Bali, Kelantan, 5. Kuala Kemaman, Terengganu, 6. Kuala Rompin, Pahang, 7. Kuala Benut, Johor, 8. Kuala Sungai Baru, Melaka, 9. Kuala Lukut, Negeri Sembilan, 10. Sg. Yu, Selangor 11. Teluk Melintang, Perak, 12. Sandakan, Sabah and 13. Bintulu, Sarawak (Table 1; Figure 1).

All samples were promptly subjected to morphological identification and verification upon collection, following the methodology outlined by Loy et al. (2000). The identified and confirmed samples were then put in a cold box before being transferred to the School of Biological Sciences, Universiti Sains Malaysia. Then, all samples were washed with running water, tapped, dried, and placed on the left side of a flat surface with a white background for maximum visibility. All fins are set up with pins to ensure correct insertion and origin. Morphometric characteristics were measured using a digital caliper (Figure 2).

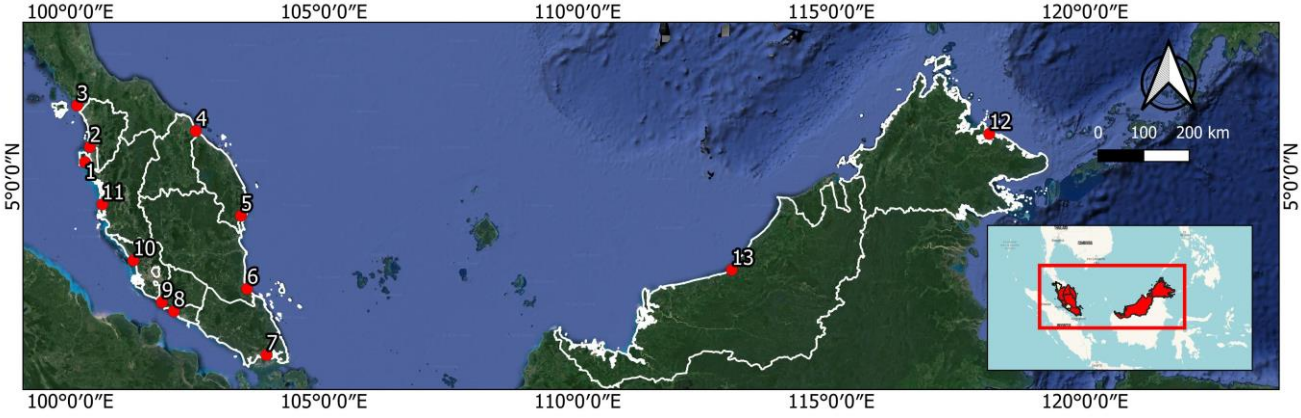

Figure 1. Sampling location of *Pampus argenteus* around Malaysian waters. 1. Batu Maung, Penang, 2. Kuala Muda, Kedah 3. Kuala Perlis, Perlis 4. Tok Bali, Kelantan 5. Kuala Kemaman, Terengganu 6. Kuala Rompin, Pahang 7. Kuala Benut, Johor 8. Kuala Sungai Baru, Melaka 9. Kuala Lukut Port Dickson, Negeri Sembilan 10. Sg. Yu Kuala Selangor, Selangor 11. Teluk Melintang (Teluk Intan), Perak 12. Sandakan, Sabah 13. Bintulu, Sarawak

Table 1. Description of sampling locations and sample size for each locality

Sampling site	Geographical location	Marine region	Coordinate Latitude; Longitude	Sample size (n)
Batu Maung, Penang (PNG)	NC	SM	5°17'5.0994"N; 100°17'14.9"E	20
Kuala Muda, Kedah (KD)	NC	SM	5°34'59.99"N; 100°22'59.99"E	20
Kuala Perlis, Perlis (PS)	NC	SM	6°23'52.44"N; 100°7'50.52"E	20
Tok Bali, Kelantan (K)	EC	SCS	5°53'51.36"N; 102°28'26.4"E	20
Kuala Kemaman, Terengganu (T)	EC	SCS	4°14'1.68"N; 103°21'49.6"E	20
Kuala Rompin, Pahang (P)	EC	SCS	2°48'2.16"N; 103°29'9.96"E	20
Kuala Benut, Johor (J)	SC	SM	1°30'1.03"N; 103°52'2.08"E	20
Kuala Sungai Baru, Melaka (M)	WC	SM	2°21'25.92"N; 102°2'21.12"E	20
Kuala Lukut Port Dickson, Negeri Sembilan (N9)	WC	SM	2°32'13.85"N; 101°48'20.56"E	20
Sg. Yu Kuala Selangor, Selangor (S)	WC	SM	3°21'17.29"N; 101°14'30.4"E	20
Teluk Melintang (Teluk Intan), Perak (PK)	NC	SM	4°27'20.52"N; 100°37'43.68"E	20
Sandakan, Sabah (SB)	BI	SS	5°50'21.84"N; 118°7'1.92"E	20
Bintulu, Sarawak (SR)	BI	SCS	3°10'16.68"N; 113°2'30.84"E	20

Note: North Coast of Peninsular Malaysia (NC), East Coast of Peninsular Malaysia (EC), South Coast of Peninsular Malaysia (SC), West Coast of Peninsular Malaysia (WC), Borneo Island (BI), South China Sea (SCS), Straits of Malacca (SM), Sulu Sea (SS), n = sample size

Geometric morphometric analyses

All samples were labeled and photographed with a digital camera (Olympus Tough TG-5) with a 12-megapixel BSI-CMOS 12.3 resolution. Images of each sample were taken on the left side only, using the same digital caliper throughout the measurement process to collect true scale information. The Tps_Utility (tpsUtil; https://life2.bio.sunysb.edu/ee/rohlf/software.html) application was used to generate an input file that the Tps_Digitise (tpsDig; https://life2.bio.sunysb.edu/ee/rohlf/software.html) data acquisition program could read. The x and y coordinates of the landmarks were captured on the digital pictures utilized as baseline data for subsequent analysis using the tpsDig2 program (ver. 2.31) (Rohlf 2017). MorphoJ (ver. 1.07) (Klingenberg 2011) reduces discrepancies in shape dimensions owing to changes in angle in digitizing images by configuring landmarks into Procrustes superimposition and generating a consensus configuration as explained by Savriama (2018).

Moreover, 13 homologous landmarks (corresponding to 13 X and 13 Y Cartesian coordinates) (Loy et al. 2000; Cantabaco et al. 2015) were chosen on digitized images of all samples such that the landmarks configurations (X, Y coordinate) on all images represent the same position (Figure 2). The centroid size is the total of all configured landmark distances from the body's center, and it is used to plot landmarks in Kendall's space shape (that is, the use of geometrical information of shape without impacts on location, scale, and rotation) (Kendall et al. 2005). A wireframe was constructed by linking landmarks with each other, measuring, and recording to analyze the shape variations.

Principal Component Analysis (PCA) was conducted to determine the maximum amount of variations in body shape to estimate species differentiation using MorphoJ Software (ver1.07) (Klingenberg 2011). Individual analyses were performed, and average values were used to analyze key variables for each individual. The significant eigenvalues from various PCAs addressed the number of variations. A Multivariate Analysis of Variance (MANOVA) was performed on Procrustes coordinates to determine the number of differences in mean body shape. Procrustes coordinates were utilized to generate Wilk's Lambda and F-ratio values, which were then employed to explain the observed variation. Resampling was performed using 1000 bootstrap iterations.

The Canonical Variate Analysis (CVA) on centroid size was used to explain differences between inter and intra-populations and performed using the MorphoJ software (ver. 1.07) (Klingenberg 2011). Procrustes ANOVA was used to test the size and shape differences significance between all populations. The CVA results were further validated by the Unweighted Pair Group Method (UPGMA), which was created on the Procrustes distance by superimposing it to infer phylogenetic signal (if any) from the occurred shape changes. The phylogenetic tree was constructed using Paleontology Statistic Software (PAST) version 4.03 (Hammer et al. 2001).

RESULTS AND DISCUSSION

Sampling data

Approximately 260 *P. argenteus* specimens were successfully collected from five different populations, namely WC, EC, NC, SC, and BI (Figure 1; Table 1).

Body size and shape variances in *P. argenteus*

A total of 22 variables were generated from 13 homologous landmarks and used to distinguish taxa based on variation in body shape among all *P. argenteus* specimens obtained. The homologous landmarks were chosen along the entire fish length to record the maximum variation in this species (Figure 2).

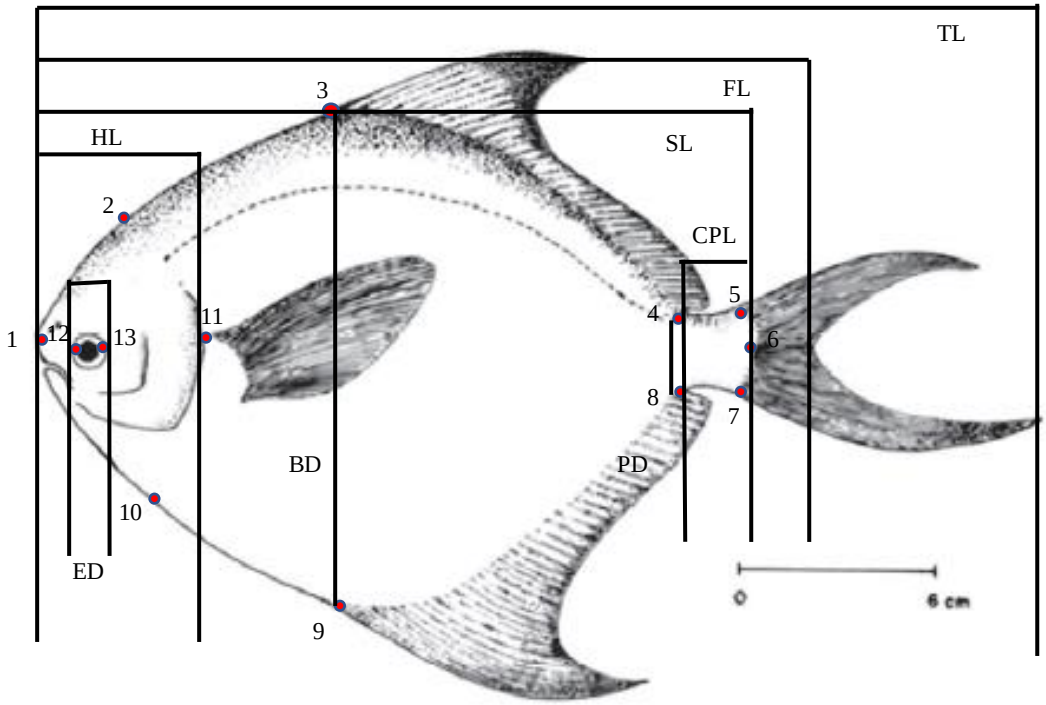

Figure 2. Locations of 13 landmarks with a description of 22 variables of *Pampus argenteus*. TL; total Length, FL; Fork Length, SL; Standard Length, BD; Body Depth, CPL; Caudal Peduncle Length, PD; Peduncle Depth, HL; Head Length. LM 1-2: Anterior tip of snout to posterior edge of the neurocranium, LM 2-3: Posterior edge of the neurocranium to anterior insertion of the dorsal fin, LM 3-4: Anterior insertion of the dorsal fin to posterior insertion of the dorsal fin, LM 4-5: Posterior insertion of the dorsal fin to point of maximum curvature of the peduncle, LM 5-6: Point of maximum curvature of the peduncle to posterior body extremity, LM 6-7: Posterior body extremity to point of maximum curvature of the peduncle, LM 7-8: Point of maximum curvature of the peduncle to posterior insertion of anal fin, LM 8-9: Posterior insertion of anal fin to anterior insertion of anal fin, LM 9-10: Anterior insertion of anal fin to insertion of the operculum on the lateral profile, LM 10-1: Insertion of the operculum on the lateral profile to anterior tip of snout, LM 13-11: Posterior margin through midline of orbit to superior insertion of the pectoral fin, LM 12-13: Anterior margin through midline of orbit to posterior margin through midline of orbit, LM 1-6: Standard length (Loy et al. 2000)

Principal Component Analysis (PCA)

The PCA of 260 *P. argenteus* specimens indicated 22 components utilized to elucidate body shape and size variations in two dimensions (x and y-axis). The first component (PC1) has the highest variance of 24.58% and eigenvalue of 0.0003, suggesting low significance [(an eigenvalue greater than 0.3 is considered significant) (Shrestha 2021)]. The first four Principal Components (PCs) are as follows: PC1 (variation in body size, body depth) with 24.58% (eigenvalue 0.0003), PC2 (variation in body depth and caudal region) with 16.6% (eigenvalue 0.0002), PC3 (variation in head region) with 12.32% (eigenvalue 0.0002) and PC4 (variation in head region and body depth) with 9.61% (eigenvalue 0.0001), respectively with a combined of all variances of approximately 63.11% (Figures 3, 4 and 5).

Based on the result in Figure 3, PC1, representing the sample's body depth and body size, showed the highest variable for overall body shape among all PCs. The second highest PCs was PC2, which appears to indicate perceptual variance in the location of the anterior insertion of the dorsal and anal fin (generally known as body depth; landmarks 3 and 9) and caudal region (landmarks 4, 5, 6, 7 and 8). A similar variation pattern is also visible in PC3, which displays variation in the location of the mouth and eye and the body depth, where the position of landmarks L1, L10, L12, and L13 are closely related. Furthermore, PC4 depicts the change in operculum insertion on the lateral profile due to landmark position transformation (landmark 10). The changes in body shape may also be seen in average specimen wireframes, as shown in Figure 4.

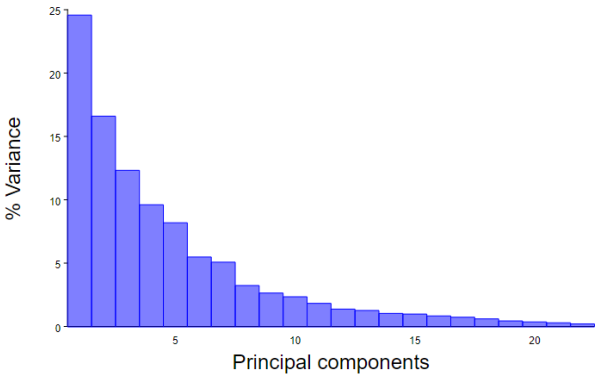

Figure 3. Values of all PCs plotted against the percentage of total variation for all samples (260 individuals) of *Pampus argenteus*

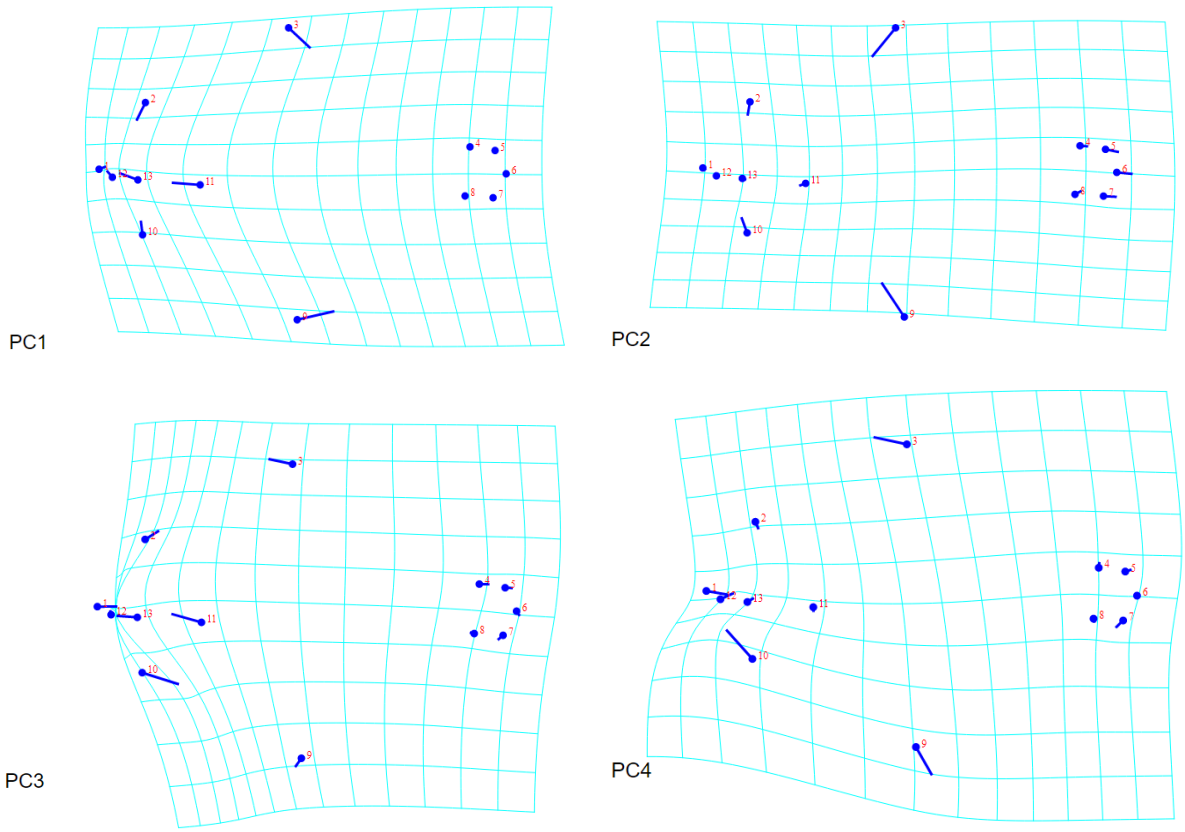

Figure 4. Visualization of shape variations from PC1 to PC4 using a wireframe to explain shape differences. PC1 demonstrates the changes in body size and depth, PC2 depicts the changes in body depth and caudal region, PC3 demonstrates changes in the mouth and eye regions (head region), and PC4 including the operculum, and it is the same as PC3

The overlapping patterns in the scatter plot of PC1 against PC2 (Figure 5) indicate that there is minimal variation in the body morphology of *P. argenteus*, with very low eigenvalues (less than 0.3) that are not significant in distinguishing individuals classified as *P. argenteus* based on the common body shape. Therefore, the averange values of all centroid size of *P. argenteus* (circle in Figure 5) from all populations (SC, NC, EC, WC, and BI) was used to get a clearer picture of the relationship between all the populations studied. The results show little segregation between all those populations considering the non-overlapping of averange value of centroid sizes (Figure 5). Figure 5 shows each sample's scatter point (centroid size) in the scatter plot of PC1 versus PC2. The circle in the scatter plots explained the averange values of all centroid size (x and y axis) of each population, which are [NC; (0.01762, -0.0099), WC; (0.004907, 0.008402), EC; (-0.01286, -0.01099), SC; (0.011098, 0.007792), and BI; (-0.01505, 0.00519)].

MANOVA was conducted to examine the disparities in mean body shape. The analysis results indicated significant variation in all examined aspects ($p < 0.0001$), and both tests yielded consistent findings. Among all currently studied samples, results revealed a significant variation ($F = 5.447$, Wilk's Lambda = 0.193, $p < 0.0001$) (Table 2). Based on the findings, the mean body shape disparities among all populations are highly significant if the F-ratio value is high. Furthermore, lower Wilks' lambda values show a better discriminating ability of body shape throughout the population. The Wilks' Lambda scale range is 0 to 1, with 0 representing total discrimination and 1 representing no discrimination (Teodoro et al. 2016). Based on the results obtained, Wilks' Lambda = 0.193, indicating discrimination among the studied population. The results obtained from MANOVA clearly show that a very significant difference is present among the *P. argenteus* population. At the same time, there is no significant difference within the population (Wilk's Lambda = 0.901, $F = 1.167$, p-value = 0.279 (Table 2). It is noteworthy that there existed statistically significant variations among the samples collected from the East Coast and North Coast ($p = 0.000$), East Coast and South Coast ($p = 0.000$), and East Coast and West Coast populations ($p = 0.001$), as indicated in Table 3. In contrast, EC and BI populations have no significant difference with p-value = 0.809. The results clearly showed populations from NC, EC, and SC, representing SM, were separated from EC and BI populations, representing SCS. The findings of this study provide clear evidence that the average body shape of *P. argenteus* exhibits significant variation, which is contingent upon their respective habitat and marine location.

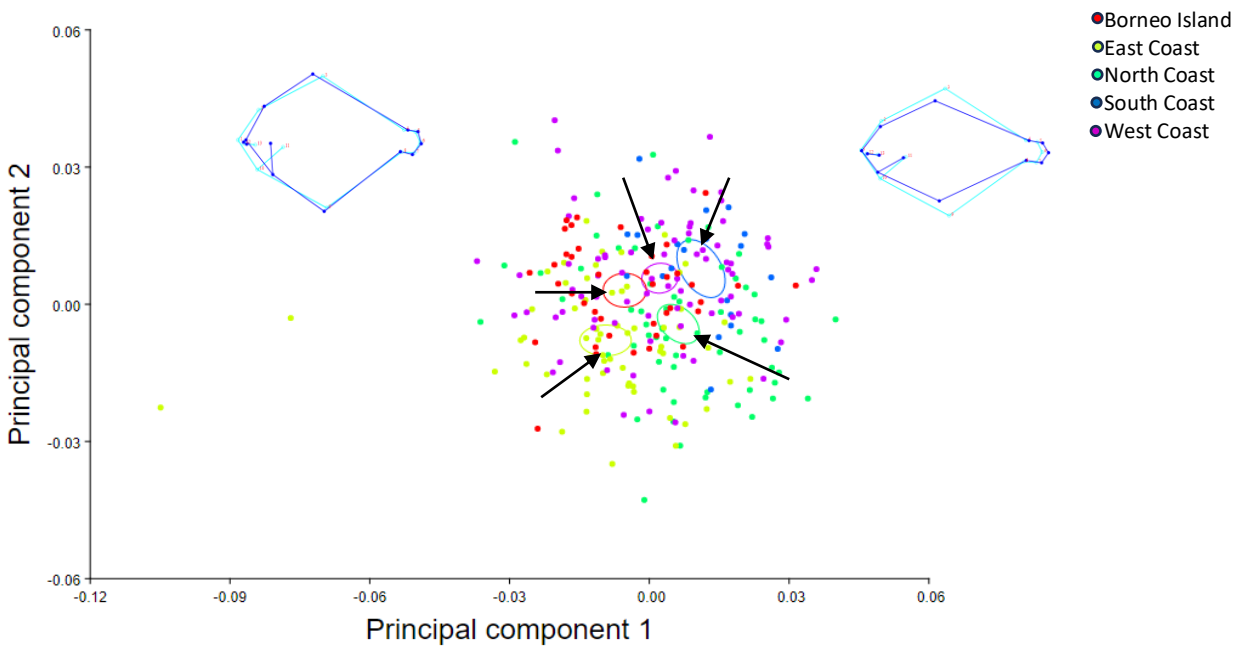

Figure 5. Principal component analysis of all *Pampus argenteus* specimens classified by region

Canonical Variate Analysis (CVA)

CVA was performed and applied to the current data of *P. argenteus* to validate the shape differences and prior group discrimination revealed by PCA analysis. CVA used new variables to minimize the within-group variation while maximizing the between-group variation. The analysis was performed on all specimens to get clear discrimination among populations by choosing 1000 permutation rounds that generated four CVs (Table 4; Figures 6 and 7). Table 4 describes the first three functions that show significant body shape differences. The maximum variation in function 1 (CV1; variation in body depth and head region) is 42.97% with a high eigenvalue of 0.92; function 2 (CV2; variation in body depth, caudal region, and head region) explains only 30.98% of body shape variations with eigenvalue of 0.66 while function 3 (CV3), 15.876% variance with eigenvalue 0.34. All four CVs had eigenvalue < 1 and 100% share the cumulative variation. The method produced identical findings as PCA but with higher support for differentiation based on eigenvalues.

Procrustes ANOVA calculated significant size and shape differences between all populations. The negative value in the x-axis of the graph explains that the population with deep body depth clusters together while the population with shallow body depth groups towards the positive zone (x-axis) of CV (Figure 7). In detail, the population of the SC, WC, and NC regions tends towards the positive zone (positive CV1 value, x-axis graph). In contrast, the population of the EC and BI tends towards the negative zone (negative CV1 value, x-axis graph). Several variations are formed based on the analysis of body shape variations from the CVA partial wrap score. CV1 describes the variation in body depth and head size region. CV2 and CV4 explain some variation in head region, caudal region, and body depth, while CV3 shows no variation among all samples (Figure 6). Procrustes ANOVA that runs on the CVA results indicates that morphological differences between all populations are highly significant ($p < 0.0001$) (Table 5). The results obtained from CVA show morphological differences between all populations of *P. argenteus* from Malaysian waters. However, the findings separated the populations into two main groups representing the marine region they belong to (Figure 7).

Table 2. Multivariate regression analysis of partial warp score and uniform centroid size of all *Pampus argenteus* specimens from all sampling sites

	F	Wilk's Lambda	p - value	df	N
Intra-population	1.167	0.901	0.279	234.000	260
Inter-population	5.447	0.193	< 0.0000	927.000	260

Note: significant p-value < 0.0001, N: Total number of samples and df: Degree of freedom.

Table 3. Multiple comparisons of samples from all populations studied

Population	NC	WC	SC	EC
NC	-			
WC	0.718	-		
SC	0.844	0.302	-	
EC	0.000*	0.001*	0.000*	-
BI	0.016*	0.208	0.008*	0.809

Note: *The mean difference is significant at p-value <0.05

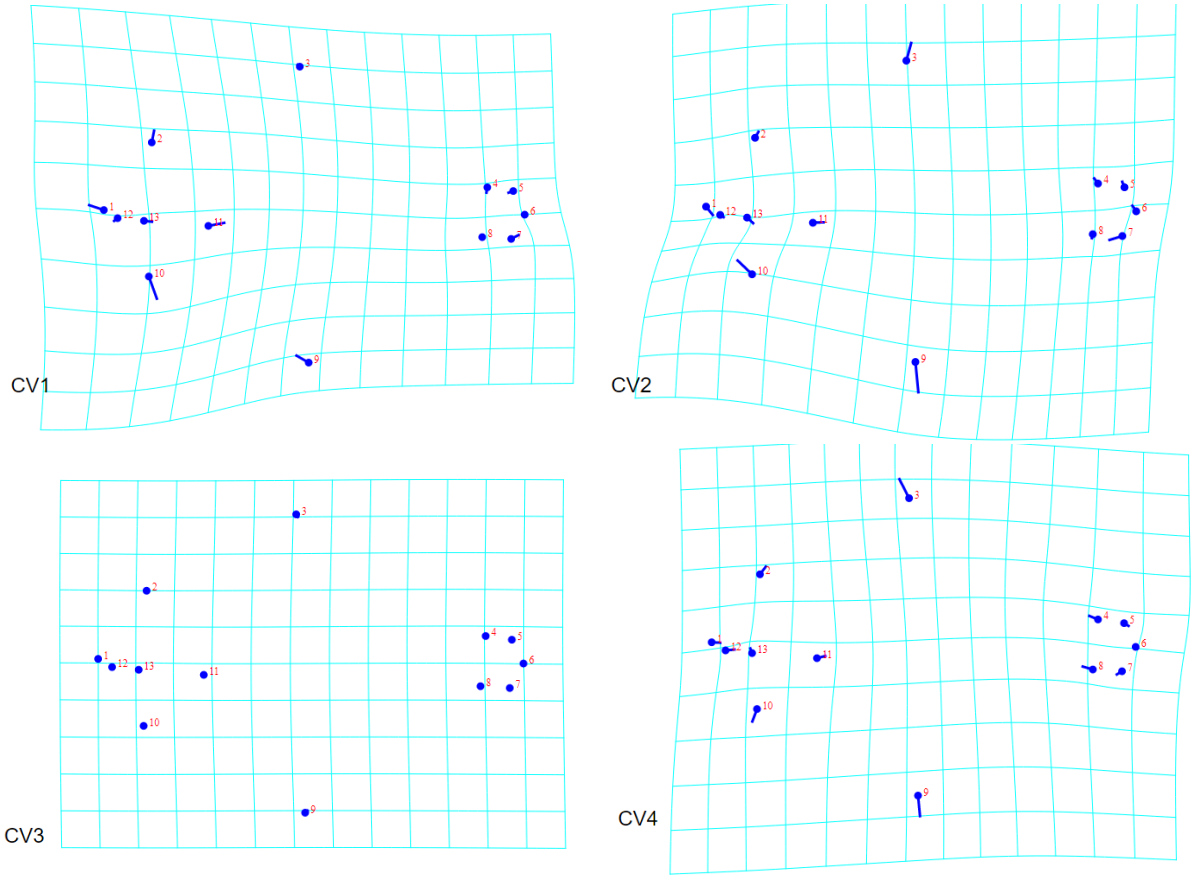

Figure 6. Visualization of shape variation along CV1 to CV4 by partial wraps along wireframe showing average shape variations. CV1 describes the variation in head size region. CV2 and CV4 explain some variation in head area and body depth, while CV3 shows no variation among all samples

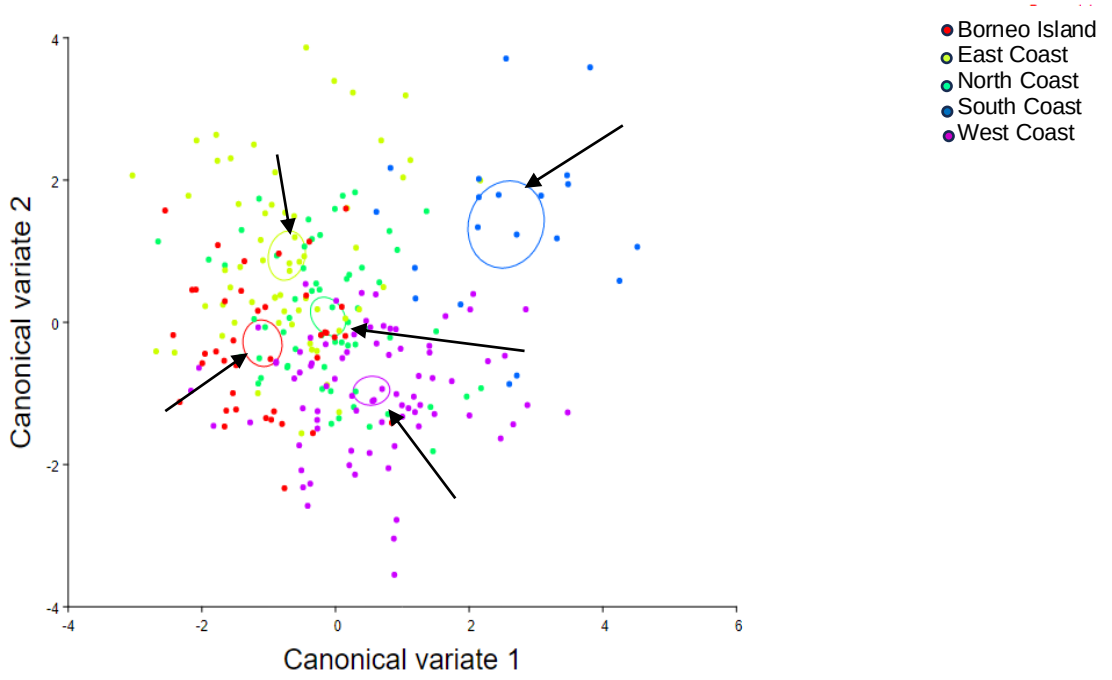

Figure 7. Canonical Variate Analysis (CVA) of five populations of *Pampus argenteus* from Malaysian waters

Pairwise differences among population

The SC was the most distinct in this research compared to all other groups (Table 6). The maximum Procrustes distance between the SC and BI is 0.0326. In contrast, a minimal distance value of 0.0129 was recorded between WC and NC, indicating that both populations had relatively similar body shapes. The p-value for all distances is 0.0001, indicating that the results are significant.

Reconstruction of evolutionary changes in *P. argenteus*

Based on the UPGMA method from the results of the CVA permutation test on the CVs, it was found that all the studied populations are closely related through their body shape and evolved in separate groups (Figure 8). The population on the SC is more diverse among the five populations studied and covers the maximum space in the canonical component. Populations from BI and EC were clustered together, explaining that they have similar morphological characteristics, while NC and WC populations clustered in another group (Figure 8). The topographic shape of the phylogenetic tree clearly shows that each group represents a different geographical sea region, namely, BI and EC represent the SCS, while the NC and WC represent the SM.

Discussion

Body shape and body size in GM are important approaches for recording morphological variations, particularly shape and size variation, as well as assessing relationships between taxa and populations of the same species based on changes in body shape (Openshaw and Keogh 2014; Imtiaz and Naim 2018). GM possesses the capacity to elucidate the underlying pattern of shape variation, which can be further correlated with additional variables, such as landmark coordinates, through the application of Procrustes superimposition (Adams and Otárola-Castillo 2013). Furthermore, GM is a powerful technique that may distinguish individuals even amongst closely related species, particularly in body structure (Cooke and Terhune 2015). The current study investigated whether GM data may be utilized to differentiate populations of *P. argenteus* in Malaysian water based on their body shape.

The GM results of this study were evident and sufficient for classifying the *P. argenteus* population into various groups based on differences in body form concerning various habitat settings. Five populations of *P. argenteus* in Malaysian waters demonstrated they were significantly different. However, the results of the PCA, CVA, and UPGMA indicated that all the samples grouped were from the same body of marine water. The findings of this study showed that populations from NC (PNG, KD, and PS) and WC (PK, S, N9, and M) were morphometrically homogeneous. This is because NC and WC belong to the SM marine region. Additionally, there was morphometric homogeneity between the populations of BI (SB and SR) and the EC (K, P, and T), both belong to the SCS maritime zone. However, individuals from SC (J) split apart from other individuals and formed a different group (Figures 5 and 7). PCA results of the GM data revealed a statistically significant outcome. However, it is worth noting that all the samples exhibited considerable overlap. This implies minimal variations in body morphology across the entire population (Figure 5). Nevertheless, CVA results (Figure 7) improved the visual representation of populations with close morphological characteristics (inter-population). Additionally, the results of PCA and CVA are further supported by the implementation of the UPGMA; this method utilizes the CVA Procrustes distance to summarise the clusters of populations effectively. This approach divides the populations into distinct groups based on their shared morphological characteristics (Figure 8).

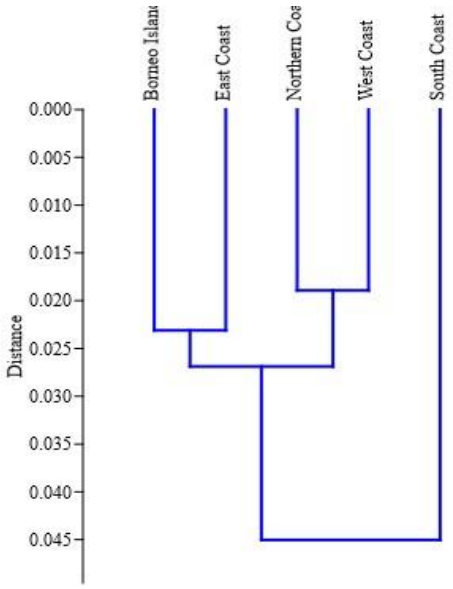

Figure 8. Reconstruction of evolutionary changes using CVA Procrustes distance of the body shape of *Pampus argenteus*

Table 4. Lists eigenvalues, variances, and cumulative based on Canonical Variate Analysis (CVA)

	Eigenvalues	Variance %	Cumulative %
CV1	0.91731592**	42.970	42.970
CV2	0.66135844**	30.980	73.950
CV3	0.33891808*	15.876	89.826
CV4	0.21718882	10.174	100.000

Note: * Eigenvalue > 0.3 showed significance; ** Eigenvalue > 0.5 were considered highly significant.

Table 6. CVA Procrustes distances among population groups of *Pampus argenteus* species

	EC	NC	SC	WC
NC	0.0179*			
SC	0.0319*	0.0232*		
WC	0.0196*	0.0129*	0.0237*	
BI	0.0158*	0.0185*	0.0326*	0.0138*

Note: * P < 0.0001 is highly significant

Table 5. Procrustes ANOVA of *Pampus argenteus* collected from Malaysian waters

Effect	SS	MS	df	F	P- value
Size					
Individual x region	1289641.213103	322410.303276	4	2.16	0.0738
Measurement error	38034737.141366	149155.831927	255	-	-
Shape					
Individual x region	0.03631603	0.0004126821	88	8.37	<.0001*
Measurement error	0.27647310	0.0000492822	5610	-	-

Note: *(P < 0.0001) highly significant; SS is the sum of squares; MS is the mean sum of squares; df is degrees of freedom, and F is the F ratio

Moreover, using the maximum number of landmarks enhances the accuracy of the data, allowing any minor variations in the body shape of the samples to be captured over the whole length of the specimens (Imtiaz and Naim 2018). In this study, 13 landmark values were computed into 22 variables. These landmark variables could fully discriminate between all individuals of the *P. argenteus* specimens in the morpho-space of PCA. Based on the presented findings, it can be observed that the initial four PCs collectively account for 63.107% of the overall body shape variation within the dataset. The study's findings comprehensively analyze the first four PCs, revealing variations in body depth, head area, and caudal region (Figures 3, 4, and 5), all of which are associated with the principal objective of adapting to environmental pressures. The locomotion, food acquisition, and fish activities vary following different environmental conditions (Imtiaz and Naim 2018). Furthermore, the study is consistent with the research conducted by Moreira et al. (2020), which examined the morphological variability of blue jack mackerel (*Trachurus picturatus* Bowdich, 1825) in the North East Atlantic and reported that there is phenotypic heterogeneity among populations, particularly in terms of body depth and caudal peduncle. Besides environmental factors, the phenotypic heterogeneity observed within species is influenced by individual genetic background (Westneat et al. 2015), culturing conditions such as temperature, hydrodynamics, and food availability (Moreira et al. 2020), as well as ecological niches that impact body shape adaptations for habitat utilization (Valladares et al. 2014). Generally, geographical differences contribute to all the aforementioned factors, thereby automatically influencing the morphological features of a species (Sajina et al. 2011). Specifically, it has been determined that the Malay Peninsular acts as a shared terrestrial barrier for many species, such as fish, whose geographical range relies on ocean currents (Binashikhbubkr et al. 2023).

The PCA results were confirmed by MANOVA analysis, which revealed that body shape had relative regional ordination. The results of the MANOVA analysis indicated significant differences in shape variation among populations (Wilk's Lambda = 0.193; F = 5.447; p < 0.000) (Table 2). However, no significant differences were observed within populations (Wilk's Lambda = 0.901; F = 1.167, p = 0.279) (Table 2). These findings also highlight that the phenotypic heterogeneity observed within *P. argenteus* in Malaysian waters is attributed to population separation, specifically geographical separation.

The positive side (positive value in PC1) of the x-axis of the graph classified individuals with extensive body depth and short caudal region. In contrast, the negative side (negative value in PC1) of the x-axis of the graph classified samples with shallow body depth and longer caudal region. Many species' morphology is well proven to be connected to their environment (Villéger et al. 2017; Fišer et al. 2018). Based on morphological investigations of *P. argenteus* populations, they are classified into five distinct populations, grouped into two main clusters representing marine regions. The SM is represented by SC, NC, and WC, which explains the clustering of individuals with similar body shape features (deep body depth and short caudal area). In contrast, the SCS is represented by BI and EC, which explains the clustering of individuals with similar body form traits (shallow body depth and longer caudal region). This demonstrates that the marine environment changes the species' physical traits based on their adaptation to the specific habitat. This statement is supported by a GM study conducted by Ismail (2018) on the Red Sea hermit crab (*Clibanarius signatus* Heller, 1861). The study found a large variation in the shape of the species' shield, which is influenced by geographical location. Likewise, Trevisan et al. (2016) have reported their work on applying GM to the carapace morphology of tiger crabs (*Aegla schmitti* Hobbs Iii, 1979*)*. Their approach successfully revealed considerable variations among all seven populations tested.

The results of this study are comparable to those reported by Moreira et al. (2020), who researched the morphology of the Ibis (*Ambassis interrupta* Bleeker, 1853) fish population. They discovered that the first four PCs showed 61.192% shape variance, which mean they had some body and head depth variations. Besides that, Binashikhbubkr et al. (2022) conducted research on the population of Kawakawa (*Eutynnus affinis* Cantor, 1849) in Peninsular Malaysia and indicated that the first four PCs accounted for 65.69% of the observed variation in body depth, head morphology, dorsal fin, anal fin, caudal fin characteristics, and overall body size. Moreover, Geiger et al. (2016) studied the morphological characteristics of barbels belonging to *Barbus* spp. Their study across different geographical areas indicated that the initial four PCs accounted for 81.3% of the body shape variation, specifically elucidating body depth alterations.

The distribution of individuals in the morpho-space represents the differences in body shape, and the clustering of the individuals into specific populations has explained that they are separated according to different body shapes (body depth, head region, and caudal region). In this study, the population's clustering pattern represents two main population groups: samples with deep body depth and shorter caudal region clusters in one group and vice versa. Based on the current study, the population from BI and EC cluster together in the morpho-space [negative-valued taxon in morpho-space- (x-axis of the graph)] and have homologous body features, such as deep body depth and a shorter caudal region. On the other hand, the population from the SC, NC, and WC cluster together in the morpho-space [positive-valued taxon in morpho-space (x-axis of the graph)] and exhibit homologous body features, including shallow body depth and a longer caudal region. Positive and negative sites in morpho-space separate the population into two major marine regions: the SCS and the SM. The changes in fish body shape are the basis for habitat diversity and ecological adaptation (Claverie and Wainwright 2014).

This study demonstrates that the body shape of the investigated *P. argenteus* can be classified into specific groups, each characterized by distinct body features. This result is most likely related to seasonal monsoons, especially in December-February and June-August. According to Liu et al. (2011), the SCS is heavily impacted by the monsoonal system, which has oceanic cyclonic circulation from December to February and anticyclonic circulation from June to August. The sampling of the *P. argenteus* for this study was done in December 2018, which was highly impacted by the monsoonal system. The theory has also been supported by Daryabor et al. (2016), who investigated the dynamics of water circulation and seasonal transport in the SCS and discovered that monsoon wind stress influences seasonal water circulation, influencing water flow. The EC water circulation patterns are mainly controlled by geostrophic currents known as ocean currents, where the Coriolis effect balances the pressure gradient force (Daryabor et al. 2016). Furthermore, the SC and SM regions are subject to wind pressure (Daryabor et al. 2016). Furthermore, water mass distribution in SM were affected by two monsoon seasons which is occurs in March and August (Mansor et al. 2023). Based on this occurrence, the wind, particularly during the monsoon, will impact the seascape and fish habitat. It is intriguing to consider the possibility that this phenomenon has indirectly influenced the morphometrics of *P. argenteus* in Malaysian waters.

Indeed, the presence of certain specimens in this study exhibiting minor differences in body size, head size, and caudal area, despite belonging to the intra-population, may elicit curiosity. This observation could potentially be associated with the gender variability exhibited by the specimen, encompassing both male and female characteristics. The present study's findings indicate that the variation in individual size was not considered, and the results demonstrate that there is no statistically significant difference ($p = 0.0738$) among all populations (Table 5). The findings of Cantabaco et al. (2015) support this observation, as they reported that females exhibited larger body sizes and higher body weights than males. These factors do not have an impact on the GM analysis. The present study's results indicate that there is a statistically significant difference ($p < 0.0001$) in the variation of individual shape across all populations (Table 5). The observed variations in the head, axial, and caudal regions of the fish examined in this study may contribute to their equilibrium and locomotion, influencing their ability to navigate water environments (Cantabaco et al. 2015). This discovery was further validated by Reece and Mehta (2013), who proposed that three regions, the head, body, and caudal area, are critical determinants in determining the variety of fish forms. Marine habitats are divided into zones based on ecological factors such as sunshine penetration, food availability, and water velocity (Mitra and Zaman 2016). The *P. argenteus* has a bilateral body that is highly compressed and oval to support its presence on muddy bottoms, brackish water, and estuaries. The variation in *P. argenteus* head shape detected in the PC zone of the wireframe explains how they adapt to different environments and habitats based on their eating habits. The species has a wide range of prey such as small crustaceans' zooplankton (copepods), algae, and semi-digested pulp that are very important in their diet (Gupta 2020). Liu et al. (2014) have reported that salps, hydromedusae, amphipods, shrimps, and other small fish groups are present in the diet of *P. argenteus* species from Kuwait water and that zooplankton and phytoplankton are the most popular food items. This statement elucidates that *P. argenteus* exhibits variations in diet based on the specific habitats they inhabit, which is influenced by ecological factors that are also reflected in their morphological characteristics. The finding mentioned above is also corroborated by Skoglund et al. (2015), whose research focused on the morphological characteristics of the head of the Arctic charr (*Salvelinus alpinus* Linnaeus, 1758). Their study revealed morphological variation following the Arctic charr's dietary preferences. In addition, Nautiyal (2018) described the influence of altered environments and dietary patterns on the catfish species' body, head, and jaw elongation (*Rita rita* Hamilton, 1822). The body shape variations observed among species are typically influenced by multiple factors, compelling them to adapt to the specific environmental conditions of their respective habitats.

The combination of morphometric data and a phylogenetic tree constructed using the UPGMA method is highly effective for presenting research findings. Numerous studies have provided evidence for the effectiveness of GM data in elucidating phylogenetic relationships. The present study has demonstrated the evolutionary patterns of *P. argenteus*, which have been represented in a phylogenetic tree (Figure 8). Interestingly, the results of the current investigation revealed that all samples could be divided into five populations and form three distinct clusters. These three different population clusters belong to geographical marine regions (SCS and SM) (Figure 8). The morphometric variability among stocks is expected due to the geographical segregation of stocks and the presence of

distinct ancestral origins. Furthermore, it has been indicated that morphological characteristics are influenced by hereditary factors, environmental factors, and their interactions (Aminan et al. 2020). The findings of this study are quite similar to those of Ramler et al. (2017), who studied Minnows (*Phoxinus*) from two different populations (Northern Italy and the Danube basin). In addition, Pauers and McMillan (2015) successfully constructed a phylogenetic tree using ecological distinctions among Cichlid fish. In addition, Killen et al. (2016) conducted a study on the morphological characteristics of Lake Trout (*Salvelinus namaycush* Walbaum, 1792). They found evidence of evolutionary relationships influenced by variations in body shape, which in turn are influenced by ecological diversity.

Morphometric variation within a fish species may arise due to various factors, including individual genetic background, culturing conditions, ecological niches, migration patterns, isolation events, environmental stressors, local adaptation, or a combination thereof. The morphological characteristics of individuals from intra-populations undergo modifications in response to their adaptive strategies, enabling their survival in novel environmental conditions. Taxonomic identification is crucial in differentiating species or populations within diverse ecological contexts. The utilization of GM proves to be a robust method for discerning the variations in body shape exhibited by *P. argenteus* within Malaysian waters. This work represents the preliminary initiative to employ a GM methodology on the *P. argenteus* species within Malaysian waters. PCA and CVA effectively demonstrated the notable differences in body morphology across the five studied populations of *P. argenteus*. Moreover, *P. argenteus* exhibits morphological heterogeneity, which can be categorized into three distinct groups based on their body shape and the marine regions they inhabit.

ACKNOWLEDGEMENTS

The authors would like to express their sincere gratitude to Universiti Sains Malaysia (USM) and the School of Biological Sciences (SBS) for providing opportunities and research facilities for this study. This work was funded by the Ministry of Higher Education Malaysia for Fundamental Research Grant Scheme (FRGS Fasa 1/2020), with project code: FRGS/1/2020/WAB11/USM/02/1.

REFERENCES

Adams DC, Otárola-Castillo E. 2013. Geomorph: An R package for the collection and analysis of geometric morphometric shape data. Method Ecol Evol 4 (4): 393-399. DOI: 10.1111/2041-210X.12035.

Aminan AW, Kit LLW, Hui CH, Sulaiman B. 2020. Morphometric analysis and genetic relationship of *Rasbora* spp. in Sarawak, Malaysia. Trop Life Sci Res 31 (2): 33-49. DOI: 10.21315/tlsr2020.31.2.3.

Binashikhbubkr K, Malik AA, Al-Misned F, Mahboob S, Naim DM. 2022. Geometric morphometric discrimination between seven populations of Kawakawa *Euthynnus affinis* (Cantor, 1849) from Peninsular Malaysia. J King Saud Univ Sci 34 (3): 101863. DOI: 10.1016/j.jksus.2022.101863.

Binashikhbubkr K, Setyawan AD, Naim DM. 2023. Population genetic structure of Kawakawa (*Euthynnus affinis* Cantor, 1849) in Malaysian waters based on COI gene. Nusantara Biosci 15 (2): 258-268. DOI: 10.13057/nusbiosci/n150213.

Cantabaco JKO, Celedio SF, Gubalani CMB, Sialana RJ, Torres MAJ, Requieron EA, Martin TTB. 2015. Determining sexual dimorphism in Bigtooth Pomfret, *Brama orcini*, in Tuka Bay, Kiamba, Sarangani Province. AACL Bioflux 8: 1009-1018.

Chen X, Wang JJ, Ai WM, Chen H, Lin HD. 2018. Phylogeography and genetic population structure of the spadenose shark (*Scoliodon macrorhynchos*) from the Chinese coast. Mitochondrial DNA Part A 29 (7): 1100-1107. DOI: 10.1080/24701394.2017.1413363.

Chong V, Lee P, Chai Ming L. 2010. Diversity, extinction risk and conservation of Malaysian fishes. J Fish Biol 76: 2009-2066. DOI: 10.1111/j.1095-8649.2010.02685.x.

Claverie T, Wainwright PC. 2014. A morphospace for reef fishes: Elongation is the dominant axis of body shape evolution. PLoS One 9 (11): e112732. DOI: 10.1371/journal.pone.0112732.

Cooke SB, Terhune CE. 2015. Form, function, and geometric morphometrics. Anat Rec 298 (1): 5-28. DOI:10.1002/ar.23065.

Cooke SJ, Martins EG, Struthers DP, Gutowsky LFG, Power M, Doka SE, Krueger CC. 2016. A moving target-incorporating knowledge of the spatial ecology of fish into the assessment and management of freshwater fish populations. Environ Monit Assess 188 (4): 239. DOI: 10.1007/s10661-016-5228-0.

Daryabor F, Ooi SH, Samah AA, Akbari A. 2016. Dynamics of the water circulations in the southern South China Sea and its seasonal transports. PLoS One 11 (7): e0158415. DOI: 10.1371/journal.pone.0158415.

Euphrasen. 1788. *Pampus argenteus*. https://www.fishbase.se/summary/491.

Fišer C, Robinson CT, Malard F. 2018. Cryptic species as a window into the paradigm shift of the species concept. Mol Ecol 27 (3): 613-635. DOI: 10.1111/mec.14486.

Franssen NR, Harris J, Clark SR, Schaefer JF, Stewart LK. 2013. Shared and unique morphological responses of stream fishes to anthropogenic habitat alteration. Proc Royal Soc B: Biol Sci 280 (1752): 20122715. DOI: 10.1098/rspb.2012.2715.

Geiger M, Schreiner C, Delmastro G, Herder F. 2016. Combining geometric morphometrics with molecular genetics to investigate a putative hybrid complex: a case study with barbels *Barbus* spp. (Teleostei: Cyprinidae). J Fish Biol 88 (3): 1038-1055. DOI: 10.1111/jfb.12871.

Gupta S. 2020. Reviews on the biology and culture of Silver Pomfret, *Pampus argenteus* (Euphrasen, 1788). Intl J Aquat Biol 8 (4): 228-245.

Hammer Ø, Harper DA, Ryan P. 2001. Paleontological statistics software package for education and data analysis. Paleontol Electron 4 (1): 1-9.

Idaszkin YL, Marquez F, Nocera A. 2013. Habitat-specific shape variation in the carapace of the crab *Cyrtograpsus angulatus*. J Zool 290 (2): 117-126. DOI: 10.1111/jzo.12019.

Imtiaz A, Naim DM. 2018. Geometric morphometrics species discrimination within the Genus Nemipterus from Malaysia and its surrounding seas. Biodiversitas 19 (6): 2316-2322. DOI: 10.13057/biodiv/d190640.

Iqbal F, Masood Z, Razzaq W, Rafique N, Din N, Zahid H, Bano N. 2015. Morphometric characteristics of silver pomfret, *Pampus argenteus* of Family Stromateidae collected from fish market of Quetta City of Pakistan. Glob Vet 15 (4): 394-396. DOI: 10.5829/idosi.gv.2015.15.04.96186.

Ismail TG. 2018. Effect of geographic location and sexual dimorphism on shield shape of the Red Sea hermit crab *Clibanarius signatus* using the geometric morphometric approach. Can J Zool 96 (7): 667-679. DOI: 10.1139/cjz-2017-0050.

Jawad LA. 2014. Caudal fin deformity in the wild silver pomfret *Pampus argenteus* collected from the Arabian Gulf coasts of Oman. Intl J Mar Sci 4 (38): 1-4. DOI: 10.5376/ijms.2014.04.0038.

Kendall FP, McCreary EK, Provance PG. 2005. Muscles: Testing and Function with Posture and Pain, ed 5 (with Primal Anatomy CD-ROM). Phys Ther 86 (2): 304-305. DOI: 10.1093/ptj/86.2.304.

Killen SS, Glazier DS, Rezende EL, Clark TD, Atkinson D, Willener AS, Halsey LG. 2016. Ecological influences and morphological correlates of resting and maximal metabolic rates across teleost fish species. Am Nat 187 (5): 592-606. DOI: 10.1086/685893.

Klingenberg CP. 2011. MorphoJ: an integrated software package for geometric morphometrics. Mol Ecol Resour 11 (2): 353-357. DOI: 10.1111/j.1755-0998.2010.02924.x.

Liu C, Zhuang Z, Chen S, Shi Z, Yan J, Liu C. 2014. Medusa consumption and prey selection of silver pomfret *Pampus argenteus* juveniles. Chin J Oceanol Limnol 32: 71-80. DOI:10.1007/s00343-014-3034-5.

Liu Q, Feng M, Wang D. 2011. ENSO-induced interannual variability in the southeastern South China Sea. J Oceanogr 67 (1): 127-133. DOI: 10.1007/s10872-011-0002-y.

LKIM. 2019. Laporan Risikan Pasaran 2019. http://portal.myagro.moa.gov.my/ms/mi/Laporan/Buku-Laporan-Risikan-Pasaran-2019.pdf

LKIM. 2020. Laporan Tahunan 2020. https://lkim.gov.my/wp-content/uploads/2022/04/LAPORAN-TAHUNAN-LKIM-2020.pdf

Lorenzen K, Cowx IG, Entsua-Mensah R, Lester NP, Koehn J, Randall R, Venturelli P. 2016. Stock assessment in inland fisheries: A foundation for sustainable use and conservation. Rev Fish Biol Fish 26: 405-440. DOI: 10.1007/s11160-016-9435-0.

Loy A, Busilacchi S, Costa C, Ferlin L, Cataudella S. 2000. Comparing geometric morphometrics and outline fitting methods to monitor fish shape variability of *Diplodus puntazzo* (Teleostea: Sparidae). Aquacult Eng 21: 271-283. DOI: 10.1016/S0144-8609(99)00035-7.

MacLeod N. 2018. The quantitative assessment of archaeological artifact groups: Beyond geometric morphometrics. Quat Sci Rev 201: 319-348. DOI: 10.1016/j.quascirev.2018.08.024.

Mansor KNAAK, Roseli NH, Ali FSM, Akhir MFM. 2023. Physical properties of seawater in Malacca Strait (Southeast Asia) during monsoon seasons. J Coast Res 39 (5): 921-932. DOI: 10.2112/JCOASTRES-D-22-00084.1.

Mitra A, Zaman S. 2016. Basics of Marine and Estuarine Ecology. Springer, New Delhi, India. DOI: 10.1007/978-81-322-2707-6.

Mohitha C. 2016. Population Genetic Structure of Silver Pomfret (*Pampus argenteus*) Along Indian Coast. ICAR-Central Marine Fisheries Research Institute. [Dissertation]. Cochin University of Science and Technology Cochin, Kerala. [India]

Moreira C, Froufe E, Vaz-Pires P, Triay-Portella R, Correia AT. 2020. Landmark-based geometric morphometrics analysis of body shape variation among populations of the blue jack mackerel, *Trachurus picturatus*, from the North-East Atlantic. J Sea Res 163: 101926. DOI: 10.1016/j.seares.2020.101926.

Nautiyal P. 2018. Diet components, dietary habits, resource and its use in the coexisting catfish species. J Inland Fish Soc India 50: 9-20.

Openshaw G, Keogh JS. 2014. Head shape evolution in monitor lizards (*Varanus*): Interactions between extreme size disparity, phylogeny and ecology. J Evol Biol 27 (2): 363-373. DOI: 10.1111/jeb.12299.

Pauers MJ, McMillan SA. 2015. Geometric morphometrics reveals surprising diversity in the Lake Malawi cichlid genus *Labeotropheus*. Hydrobiologia 748 (1): 145-160. DOI: 10.1007/s10750-014-1941-2.

Ramler D, Palandačić A, Delmastro GB, Wanzenböck J, Ahnelt H. 2017. Morphological divergence of lake and stream *Phoxinus* of Northern Italy and the Danube basin based on geometric morphometric analysis. Ecol Evol 7 (2): 572-584. DOI: 10.1002/ece3.2648.

Reece JS, Mehta RS. 2013. Evolutionary history of elongation and maximum body length in moray eels (Anguilliformes: Muraenidae). Biol J Linn Soc 109 (4): 861-875. DOI: 10.1111/bij.12098.

Rohlf FJ. 2017. TpsDig, Digitize Landmarks and Outlines (Version 2.31). Stony Brook, New York.

Sajina A, Chakraborty S, Jaiswar A, Pazhayamadam D, Sudheesan D. 2011. Stock structure analysis of *Megalaspis cordyla* (Linnaeus, 1758) along the Indian coast based on truss network analysis. Fish Res 108 (1): 100-105. DOI: 10.1016/j.fishres.2010.12.006.

Savriama Y. 2018. A step-by-step guide for geometric morphometrics of floral symmetry. Front Plant Sci 9: 1433. DOI:10.3389/fpls.2018.01433.

Shrestha N. 2021. Factor analysis as a tool for survey analysis. Am J Appl Math Stat 9 (1): 4-11. DOI: 10.12691/ajams-9-1-2.

Skoglund S, Siwertsson A, Amundsen PA, Knudsen R. 2015. Morphological divergence between three Arctic charr morphs–the significance of the deep-water environment. Ecol Evol 5 (15): 3114-3129. DOI: 10.1002/ece3.1573.

Teodoro S, Terossi M, Mantelatto F, Costa R. 2016. Discordance in the identification of juvenile pink shrimp (*Farfantepenaeus brasiliensis* and *F. paulensis*: Family Penaeidae): an integrative approach using morphology, morphometry and barcoding. Fish Res 183: 244-253. DOI: 10.1016/j.fishres.2016.06.009.

Trevisan A, Marochi MZ, Costa M, Santos S, Masunari S. 2012. Sexual dimorphism in *Aegla marginata* (Decapoda: Anomura). Nauplius 20: 75-86. DOI: 10.1590/S0104-64972012000100008.

Trevisan A, Marochi MZ, Costa M, Santos S, Masunari S. 2016. Effects of the evolution of the Serra do Mar mountains on the shape of the geographically isolated populations of *Aegla schmitti* Hobbs III, 1979 (Decapoda: Anomura). Acta Zool 97 (1): 34-41. DOI: 10.1111/azo.12102.

Valladares F, Matesanz S, Guilhaumon F, Araújo MB, Balaguer L, Benito-Garzón M, Naya DE, Nicotra AB, Poorter H, Zavala MA. 2014. The effects of phenotypic plasticity and local adaptation on forecasts of species range shifts under climate change. Ecol Lett 17 (11): 1351-1364. DOI: 10.1111/ele.12348.

Villéger S, Brosse S, Mouchet M, Mouillot D, Vanni MJ. 2017. Functional ecology of fish: Current approaches and future challenges. Aquat Sci 79: 783-801. DOI: 10.1007/s00027-017-0546-z.

Westneat DF, Wright J, Dingemanse NJ. 2015. The biology hidden inside residual within-individual phenotypic variation. Biol Rev Camb Philos Soc 90 (3): 729-743. DOI: 10.1111/brv.12131.

Zhang C, Fan Y, Ye Z, Li Z, Yu H. 2017. Identification of five *Pampus* species from the coast of China based on sagittal otolith morphology analysis. Acta Oceanol Sin 36 (2): 51-56. DOI: 10.1007/s13131-017-0982-6.